# Susceptibility Enhanced Imaging of Bioengineered Constructs for an Artificial Pancreas

S. C. Grant[1], S. J. Blackband[1], H. Mao[2], J. Oca-Cossio[3], N. E. Simpson[3], I. Constantinidis[3]

[1]Neuroscience, University of Florida McKnight Brain Institute, Gainesville, FL, United States, [2]Radiology, Emory University School of Medicine, Atlanta, GA, United States, [3]Medicine, Division of Endocrinology, University of Florida College of Medicine, Gainesville, FL, United States

**Introduction:** In recent years, the increased usage of paramagnetic magnetic contrast agents in the field of MR imaging has been spurred by cellular and molecular imaging initiatives (1). These efforts have included the detection of single mammalian cells at relatively high image resolutions through the uptake of superparamagnetic iron oxide (SPIO) particles in lymphocytes (2) and cancer cells (3) for the purpose of cell tracking. Additionally, iron nanoparticles have demonstrated potential utility in detecting immune response during chemically-induced pancreatic insulitis (4). To date, most investigations have focused on the relaxing effects of iron oxide particles on T2 or T2* contrast. Thus, these studies have championed the negative contrast attributes of iron oxide labeling. However, at least two studies have utilized the dipolar field distortion induced by the magnetic susceptibility of iron oxide particles to generate positive contrast for passive MR-guided endovascular interventions (5) and *in vitro/ex vivo* cell tracking (6). This "white-marker" technique based on paramagnetic susceptibility is uniquely interesting outside of the central nervous system, particularly for imaging applications involving the abdomen. The focus of this study is to evaluate the potential of positive contrast susceptibility imaging of iron oxide-labeled bioengineered constructs (namely an artificial pancreas) intended for transplantation in the peritoneal cavity.

**Methods:** *Fabrication of the construct and MION exposure:* The bioartificial pancreas consists of insulin-producing murine insulinoma cell lines encapsulated in alginate microbeads. For this study, a high mannuronic alginate (2% MVM consisting of 36% guluronic acid/67% mannuronic acid) gelled in 100-mM $CaCl_2$ was used to encapsulate βTC-tet cells in beads having a diameter of roughly 500 μm. Prior to imaging, cell-loaded beads were incubated for 20 hours in Dulbecco's modified Eagle's medium (DMEM) supplemented with 15% horse serum, 2.5% bovine serum, 1% penicillin-streptomycin and L-glutamine to a final concentration of 6 mM. Monocrystalline iron oxide nanoparticles (MIONs) were chosen as the paramagnetic contrast agents. In all test groups, a 10-mM citrate-buffered MION was used (7). Three bead preparations were generated in which: (a) cells were loaded with MION prior to bead formation (MION-CELL), (b) MVM alginate was exposed to MION prior to bead formation (MION-MVM), and (c) non-MION exposed controls (SHAM). The MION-CELL prep was labeled by adding 0.25 mL of the 10-mM MION solution to 20 mL of DMEM. The MION-MVM prep was created by mixing 5 mL of 2% alginate solution with 62.5 μL of the MION solution. For the SHAM group, 0.25 mL of citrate buffer was added to 20 mL of DMEM.

*MR imaging*: Following incubation, a small sampling of beads from each prep were washed in fresh DMEM and loaded individually into glass capillaries with DMEM. These capillaries were placed within a specially built solenoidal microcoil that allowed several beads to be analyzed simultaneously. All MRI data were acquired using a vertical 17.6-T magnet equipped with a Bruker Avance console and Micro2.5 gradients. Multi-slice 2D gradient echo (GE) images were acquired at echo times (TE) varying from 5-30 ms (NEX = 2; MTX = 128x32; BW = 28 kHz; TR = 1 s; FOV = 6.8x1.7 mm; slice = 0.10 mm). Positive contrast susceptibility imaging was achieved by reducing the slice refocusing gradient by 30% and 40% in subsequent experiments. Modulations of the positive susceptibility contrast were examined by varying TE and BW. In addition to positive contrast datasets, appropriately sampled, high resolution (27-μm isotropic) 3D GE images and T2- and diffusion-weighted spin echo (SE) images were acquired for the calculation of T2*, T2 and ADC respectively. All three preps were imaged once a week for 21 days. Correlative histology and an analysis of metabolic function was conducted for each time point.

**Results and Discussion:** These *in vitro* results display intriguing patterns of positive contrast resulting from the dipolar field distortions of the MION particles. Figure 1 displays a single slice from the MION-CELL prep images. Standard GE images display an increased heterogeneity and T2* weighting compared to the SHAM results (Fig. 3). This heterogeneity is particularly evident in the positive contrast images, for which the MION-CELL images display striking pinpoint contrast through the volume of the bead. The MION-MVM prep (Fig. 2) shows strong and uniform T2*-weighted contrast in standard GE images. In positive contrast images, the MION-MVM beads display a weaker distortion profile representative of a spherical susceptibility perturbation. Surprisingly, the SHAM prep also displays significant contrast enhancement with the positive susceptibility technique (Fig 3.). Although not as strong as in the MION-MVM beads, the positive contrast of the SHAM beads represents a homogeneous perturbation at this early time point (strongest contrast at high TE/low BW). Unlike the MION preps, the SHAM beads display increasing heterogeneity in T2, ADC and positive contrast over time as cells proliferate. Additionally, as seen previously (7), the presence of MION inside or outside of the cells showed no adverse effects on cell proliferation or metabolism as assessed by MR and biochemical techniques.

In conclusion, it is evident that positive contrast susceptibility techniques, particularly at high field, show great potential for imaging implanted cellular constructs.

***Fig. 1*** *2D GE images of MION-CELL Prep: Day 1*
*Top row: TE = 6ms; Bottom row: TE = 24ms*

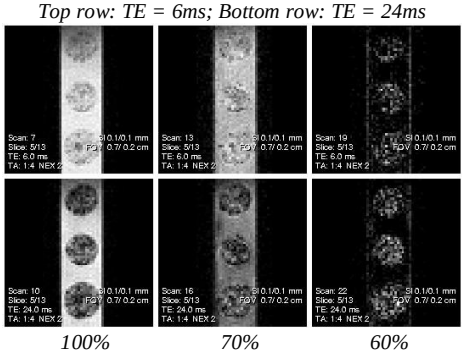

*100%* *70%* *60%*
*Slice Refocusing*

***Fig. 2*** *2D GE images of MION-MV Prep: Day 1*
*Top row: TE = 6ms; Bottom row: TE = 24ms*

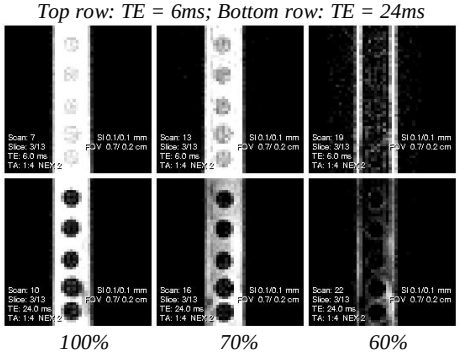

*100%* *70%* *60%*
*Slice Refocusing*

***Fig. 3*** *2D GE images of SHAM Prep: Day 1*
*Top row: TE = 6ms; Bottom row: TE = 24ms*

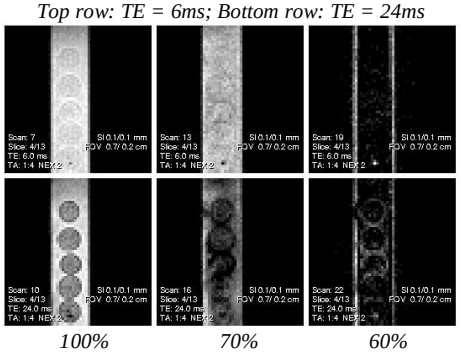

*100%* *70%* *60%*
*Slice Refocusing*

**References**

1. Bulte JWM and Kraitchman DL, NMR Biomed. 2004. 17: 484-99.
2. Dodd SJ et al., Biophys. Journ. 1999. 76: 103-9.
3. Foster-Gareau P, et al., Magn. Reson. Med. 2003. 49: 968-71.
4. Moore A, et al., Magn. Reson. Med. 2002. 47: 751-8.
5. Seppenwoolde JH et al., Magn. Reson. Med. 2003. 50: 784-90.
6. Coristine AJ, et al., Proc. 12th ISMRM. 2004: 163.
7. Oca-Cossio J, et al., Biochem. Biophys.Res. Comm. 2004. 319: 569-75.

**Acknowledgements**

Funding provided by the NIH (P41-RR16105, R01 DK56890, R01 DK47858), the National High Magnetic Field Laboratory & the UF McKnight Brain Institute (AMRIS). The authors also would like to thank AJ Coristine and BK Rutt for useful discussions.